PERGAMON

Corrosion Science 41 (1999) 1639–1664

CORROSION SCIENCE

Electrochemical investigation of the influence of nitrogen alloying on pitting corrosion of austenitic stainless steels

R.F.A. Jargelius-Pettersson*

Swedish Institute for Metals Research, Drottning Kristinas väg 48, 114 28 Stockholm, Sweden

Received 17 September 1998; accepted 18 January 1999

Abstract

A systematic investigation has been performed of the influence of nitrogen alloying on the pitting corrosion of austenitic stainless steels. The alloys investigated had a base composition of 20% Cr–25% Ni with 0% or 4.5% Mo. The nitrogen level was varied up to the solid solubility limit at approximately 0.2%. The critical temperature for pitting corrosion increases with nitrogen additions and the effect is more marked in the molybdenum-alloyed steels, indicating a synergistic interaction between the two alloying elements. A number of investigations have been performed to elucidate the mechanisms for the influence of nitrogen on pitting corrosion and for Mo–N synergism.

Keywords: Stainless steel; Pitting; Repassivation

1. Introduction

The influence of nitrogen alloying on the corrosion properties of stainless steels has received much attention in recent years, and has also been the subject of a number of reviews [1–5]. There is fairly universal agreement than nitrogen additions improve the pitting corrosion resistance of austenitic stainless steels; increasing the pitting potential in aqueous chloride solutions [6–13] or decreasing the weight loss in immersion testing in $FeCl_3$ [7, 9, 14, 15]. Similar beneficial effects have also been reported for duplex steels [16–18], austenitic welds [19] Fe–N alloys [4, 20], tool steels [21] and low-alloy steels [22]. The concept of nitrogen–molybdenum synergy, whereby greater beneficial

* Corresponding author. Tel.: +0046-8-440-48-00; Fax: +0046-8-440-45-35.

0010-938X/99/$ - see front matter
PII: S0010-938X(99)00013-X

effects are attained by nitrogen additions in the presence of molybdenum, is also widely-acknowledged [1, 9, 14, 23–31]. Only in exceptional cases have negative effects of nitrogen alloying on pitting resistance been reported [32, 33].

There is less consensus regarding the effect of nitrogen alloying on general corrosion resistance or active dissolution. In an early work, Osozawa and Okato [7, 8] demonstrated that nitrogen had a smaller beneficial effect on the critical current density for passivation in 0.5 M H_2SO_4 + 0.05 M NaCl than on the pitting potential when compared to other alloying elements. Nitrogen alloying has been shown in several studies [2, 10, 27, 34, 35] to decrease the critical current density in HCl. For 17 Cr–12 Ni–2.5 Mo steels, the largest effect has been seen around 4 M HCl in stagnant solution [2] or 5 M for rotating disc electrodes [34]. Similar beneficial effects have been noted for various steels in 0.1 M HCl + 0.4 M NaCl [12] and 7.5 M H_2SO_4 [13]. However, nitrogen has also been reported to have a negligible effect on the active peak for 6% Mo austenitic stainless steels in 0.5 M HCl + 2 M NaCl [27] and for 17 Cr–13 Ni steels in 0.5 M H_2SO_4 [36].

In terms of passive film properties, nitrogen has been observed to decrease the passive current density [10, 12] or to have a negligible effect [6, 27]. A decrease in passive film capacity has been noted for N-implanted 18–8 steels in 0.5 M NaCl [13] but the converse for nitrided iron in 0.01 M H_2SO_4 + 0.99 M Na_2SO_4 [37]. There is, however, a general consensus that nitrogen accelerates repassivation, both for Fe–N alloys [4, 20, 37] and for stainless steels [8, 27], particularly in the presence of chloride [38].

There has been extensive discussion in the literature about nitrogen's effect on corrosion properties and the proposed mechanisms may be divided into the following categories:

1.1. Microstructural effects

Chernova [39] attributed the beneficial effect of nitrogen to structural homogenisation caused by the elimination of delta ferrite, and Janik Czachor [6] observed that nitrogen modified the ratio or composition of carbide phases which acted as pit initiation sites. In sensitised stainless steels [40, 41] and in welds, particularly of duplex stainless steels [42], microstructural modification is often the dominant effect of nitrogen on corrosion properties. However, these arguments are not readily applicable to austenitic stainless steels which have a homogenous, single-phase structure.

1.2. Electrochemical ammonium formation

Osozawa and Okato [8] were the first to detect the presence of NH_4^+ following dissolution of nitrogen-containing stainless steels in pitting tests in 20% $FeCl_3$. They proposed the idea that the formation of ammonium ions consumes protons and thereby increases the pH in incipient pits and promotes repassivation. This electrochemical nitrogen dissolution reaction may be represented as:

$$[N] + 4H^+ + 3e^- \rightarrow NH_4^+. \quad (1)$$

Subsequent works [22, 30, 35, 43–45] have confirmed NH_4^+ formation in a variety of media and have demonstrated that the NH_4^+ generation rate increases with the amount of nitrogen in the steel [44] and decreases with increasing applied potential [35]. In XPS studies, NH_4^+ (or NH_3) has been detected at passive [1, 11, 27, 29, 46, 47], active [1, 48, 35] and transpassive [1] potentials for stainless steels. Similar surface analysis results have also led to the suggestion that the same mechanism may even be operative for aluminium implanted with nitrogen [49].

1.3. Ammonium formation from nitride dissolution

Willenbruch et al. [50] noted that nitriding caused a remarkable reduction in the active dissolution of chromium and suggested that surface CrN may act as a precursor to passive film formation and also form NH_4^+/NH_3 on dissolution via the reaction:

$$2CrN + 3H_2O \rightarrow Cr_2O_3 + 2NH_3 \text{ (ligands)}. \quad (2)$$

It was also pointed out [51] that this would counteract the drop in surface pH which would otherwise be a consequence of metal hydration or oxide formation. Experimental evidence for the possibility of such a mechanism is provided by the work of Kolotyrkin et al. [43] who observed Cr_2N precipitates to form NH_4^+ on dissolution. However, they also noted that such nitrides were very reactive and resulted in a more rapid release of chromium than did dissolution of the pure metal.

A mechanism based on ammonium formation from chemical dissolution of nitrides circumvents objections [10, 11, 52] to the mechanism of Section 1.2 on the grounds that eq. (1) is a cathodic reaction which should cease at sufficiently anodic potentials, behaviour which is difficult to reconcile with the observation that the effect of nitrogen is larger in molybdenum-alloyed steels for which the pitting potential is higher [10, 52].

1.4. Nitrate formation

The inhibiting effects of nitrates are widely recognised [14, 53–55] and Truman [53] suggested speculatively that nitrate formation during dissolution could inhibit pit growth. Kamachi Mudali [19] proposed that NH_4^+ from eq. (1) could form inhibiting species, such as NO_2^- or NO_3^-, by processes such as:

$$NH_4^+ + 2H_2O \rightarrow NO_2^- + 8H^+ + 6e^-. \quad (3)$$

In this context, it may however be noted that the widely-accepted mechanism [52, 10, 54, 55] for the inhibiting role of nitrate is itself via acid consumption and ammonium formation, i.e. [54, 55]:

$$NO_3^- + 10H^+ + 8e^- \rightarrow 3H_2O + NH_4^+. \quad (4)$$

1.5. Nitrogen incorporation in the passive film

The concept that nitrogen is incorporated in and improves the properties of the passive film was suggested in early works by Truman [9] and Bandy [14] and also invoked by Song [13] to explain impedance data. Indications of a nitride in the passive film have been presented by Sadough Vanini et al. [36], who argued that dispersed particles of chromium nitride in the passive film were responsible for the detrimental effect of nitrogen on passivation observed in their investigation. However, other surface analytical studies [1, 10–12, 27, 46–48, 56–58] have provided little evidence of significant amounts of nitrogen within the passive film.

1.6. Nitrogen enrichment beneath the passive film

Nitrogen enrichment has been observed at the metal–film interface in a number of works. Lu et al. [27, 56] first reported an apparent nitrogen concentration at the metal side of the interface which was seven times the level in the bulk alloy and concluded, from XPS binding energy data, that this was in an uncharged form. Later works by Clayton et al. [1, 10–12, 48, 57, 58] confirmed interfacial nitrogen enrichment but identified this as a negatively-charged state, such as a nitride phase. They found evidence of Ni–Mo–N synergism [12, 51, 57, 58] and attributed this to the formation of a stable mixed nitride surface layer, such as Ni_2Mo_3N.

In contrast, Olefjord et al. [59] suggested, on the basis of XPS studies, that a thin intermetallic layer formed on the active surface or beneath the passive film may be responsible for improving corrosion properties. Modelling was used [48] to predict the occurrence of Ni–Mo and weaker Ni–Cr bonding and it was suggested that nitrogen may increase the strength of this bonding. Olefjord and Wegrelius [47] found interfacial nitrogen to correspond to 12–20% of an atomic layer but argued against the formation of chromium nitrides on thermodynamic grounds (energetically unfavourable compared to chromium oxide) and against Ni_2Mo_3N, since the measured molybdenum content was too low.

A different interpretation of the role of interfacial nitrogen accumulation was made by Grabke [4]. A comparison with AES, XPS and LEED analysis of surface segregation on Fe–N single crystals at elevated temperatures [60] was used to demonstrate that the interfacial nitrogen species is negatively charged. On this basis, he proposed that nitrogen decreases the potential gradient across the film and repels chloride ions, also that desorption of aggressive ions is induced by segregated $N^{\delta-}$ just after the local failure of the passive film. It was further suggested that this negatively charged nitrogen probably converts directly to ammonium via the reaction:

$$N_3^- + 4H^+ \rightarrow NH_4^+. \quad (5)$$

1.7. Anodic segregation of nitrogen at actively dissolving surfaces

The idea that significant transient anodic segregation of nitrogen may occur during dissolution was first proposed by Newman et al. [27] and subsequently demonstrated

in a number of surface analytical studies [1, 35, 48]. Bandy et al. [10] put forward two reasons why both nitrogen and molybdenum should accumulate on anodically dissolving surfaces: that they are thermodynamically more noble than iron and that their dissolution reactions are slow, multi-electron processes. It was also pointed out by these authors and by Newman and Shahrabi [2] that, because the nitrogen dissolution reaction eq. (1) is cathodic, nitrogen will accumulate at a dissolving surface, particularly at the higher potentials to which molybdenum displaces dissolution. They therefore suggested that nitrogen will tend to accumulate at active surface sites, such as kink and step sites, and stifle active dissolution. Newman and Shahrabi [2] took this argument a step further in claiming this could lead to a fundamentally different passivation process, associated with nitrogen blockage of dissolution sites, which was both reversible and insensitive to solution flow and which could occur below the potential at which Cr_2O_3 forms.

1.8. Modification of the dissolution behaviour of Fe, Cr or Mo

Nitrogen has frequently been reported to accelerate the anodic dissolution of iron in acidic solutions [4, 20, 38, 50, 58, 61], although the converse has been reported in neutral solutions [38, 61]. It has also been demonstrated to stimulate the selective dissolution of iron from stainless steels [12]. Conversely, nitriding pure chromium decreases the dissolution rate [16, 38, 50] and may even completely eliminate the active peak [50] while, in steels, nitrogen can enhance surface accumulation of chromium [22] and suppress its release into solution [16]. The dissolution of molybdenum is largely unaffected in the active range [50] by nitriding but suppressed at transpassive potentials [28].

These observations have been used to support the idea that nitrogen modifies the surface composition of stainless steels and thereby facilitates repassivation. Lu et al. [29] pointed out that the higher stability of Cr and Mo nitrides in acidic solutions than in neutral solutions may accelerate the anodic segregation of beneficial elements during localized corrosion, therefore building up a more resistive surface layer at pit sites. They also suggested [28, 29] that nitrogen can inhibit the transpassive dissolution of molybdenum, possibly by nitride formation, and effectively retain Mo in the passive film. Surface analytical studies have, however, provided somewhat conflicting evidence. Clayton et al. [1] found nitrogen to increase the concentration of Cr and Mo in the passive film and noted that Ni, Mo and N all promoted the selective dissolution of iron; but Olefjord and Wegrelius [47] observed no effect of nitrogen on either the film or the underlying metallic composition.

1.9. Salt film formation

In sulphate solutions, Clayton et al. [1, 11] suggested that NH_4^+ may form an ammonium sulphate layer which may act as a temporary prepassive barrier between the metal and the solution. In a related vein, Newman and Ajjawi [55] have

demonstrated that nitrate inhibition of stainless steels in chloride solutions involves salt film formation.

1.10. Removal of free chlorine

Ives et al. [62] suggested that in chlorinated water systems, ammonium may react with free chlorine to form combined chlorine species which are less effective oxidants than free chlorine.

1.11. Synergistic effects

In view of the recognised importance of nitrogen–molybdenum synergism in improving localised corrosion resistance, surprisingly few papers have addressed possible mechanisms for this interaction. The first suggestion, put forward by Newman et al. in 1984 [27], was that Mo and N may form a surface array which inhibits further dissolution. This idea of cosegregation is also implicit in the arguments in Section 1.8 above, namely that nitrogen modifies the dissolution and therefore surface concentration of alloying elements in stainless steels also, in the reasoning from Section 1.6, that nitride or nitrogen-promoted intermetallic surface bonding occurs.

Arguments based on solution chemistry have also been put forward. Lu et al. [29] suggested that the formation of NH_3 ligands raises the local pH and favours the formation of molybdate, which enhances the passivity of stainless steels. Olsson [46] showed evidence of interaction between highly mobile Mo and N ions near the passive layer region and formation of a passive layer which is independent of the underlying phase. His tentative explanation of the synergistic interaction was that not only does nitrogen buffer the pH and stabilise molybdates, but also that molybdates would assist in the formation of ammonium, since the presence of molybdate in the passive film is an important parameter for the deprotonation of the film [63].

Bandy et al. [10] and Newman and Shahrabi [2] suggested that synergistic interaction is observed because molybdenum displaces metal dissolution (and pitting) to higher potentials. At sufficiently high potentials, nitrogen will accumulate at kink sites because the dissolution reaction eq. (1) is cathodic, and it may be that the cross-over point of the anodic dissolution and nitrogen reduction reactions is thereby shifted to current densities below the critical value for pit initiation. Likewise, Olefjord and Wegrelius [47] suggested that enrichment of Mo at the metal–electrolyte interface of initiated pits decreases the dissolution rate to such an extent that formation of NH_3/NH_4^+ can compensate for the pH drop.

Finally, Newman and Shahrabi [2] speculatively suggested that there may be a specific interaction between Mo and N, analogous to molybdenum's role in biological nitrogen fixation.

The aim of the present work [64, 65] is to contribute to the elucidation of nitrogen mechanisms via electrochemical investigation of a series of experimental alloys with

systematic variation in Mo and N contents. Pitting, passive film development and dissolution behaviour in acidic chloride solutions (which have a bearing on the dissolution conditions inside a pit or crevice) are examined.

2. Experimental

2.1. Materials and heat treatment

The compositions of the eight experimental alloys investigated are listed in Table 1. K1–K3 and L1–L3 were produced as laboratory heats, then forged, hot rolled and cold rolled to produce 3 mm strip. They were annealed for 20 min at 1100°C and brine-quenched to give an austenitic structure, free from second phase precipitates and with a final grain size of 60–70 μm. The low nitrogen contents in K0 and L0 were attained by denitriding in hydrogen for 72 h at 1200°C, followed by cold rolling to reduce the grain size and final annealing for 20 min at 1100°C. For corrosion testing, specimens were wet surface ground to 600 mesh SiC paper, unless otherwise specified. For pitting tests, specimens were allowed to passivate in air for at least 18 h prior to testing.

2.2. Pitting corrosion

The critical temperature for pitting corrosion was determined in 0.2 M NaCl at a potential of +600 mV SCE by raising the temperature by 2°C every 15 min until an irreversible current increase indicated the onset of stable pitting. Specimens had dimensions $40 \times 15 \times 3$ mm and were suspended in a specimen holder in which all specimen contacts were under an argon bubble and thus not susceptible to crevice corrosion. The exposed area was approximately 10 cm^2, this included both the flat surface and edges of the specimen. Pit initiation sites were investigated using immersion testing of polished specimens in a solution comprising 8 g $AlCl_3$ and 8 g $FeCl_3$ in 50 ml glycerol + 50 ml ethanol [66]. The solution temperature was 20°C for the K

Table 1
Composition of the alloys investigated (wt.%).

	C	Si	Mn	P	S	Cr	Ni	Mo	N
K0	0.003	0.53	1.31	0.010	<0.003	20.14	24.75	0.08	0.010
K1	0.014	0.53	1.31	0.010	<0.003	20.14	24.75	0.08	0.064
K2	0.014	0.55	1.43	0.009	<0.003	20.03	24.87	0.04	0.130
K3	0.013	0.55	1.43	0.010	<0.003	19.96	24.90	0.04	0.180
L0	0.003	0.54	1.42	0.010	<0.003	19.20	24.86	4.50	0.015
L1	0.020	0.54	1.42	0.010	<0.003	19.85	24.86	4.50	0.061
L2	0.015	0.49	1.45	0.009	<0.003	19.87	24.95	4.55	0.130
L3	0.014	0.54	1.44	0.009	<0.003	19.83	24.99	4.59	0.210

series and 60°C for the L series, this resulted in pit initiation times of approximately 5 min. Pitting potentials in 1 M NaCl were determined at various temperatures using a potential scan rate of 20 mV/min from the corrosion potential. In this case, only 1 cm^2 of the flat surface was exposed and a combination of passivation and lacquering was used to avoid crevice corrosion.

2.3. Passive and active corrosion

Passive current density measurements were conducted at +150 and +600 mV SCE in 0.5 M NaCl acidified to pH = 3 by addition of HCl, also at +150 mV SCE in 0.9 M NaCl + 0.1 M HCl. The solutions were deaerated with argon for 160 h before each experiment; the specimen dimension and holder were the same as for the CPT measurements. Electrochemical noise data were obtained for smaller specimens (1 cm^2) under the same conditions and transformed to the frequency domain using FFT analysis. Polarisation curves were obtained in various concentrations of H_2SO_4 + HCl using a potential scan rate of 20 mV/min from −700 or −550 mV SCE on specimens of area 1 cm^2. In HCl solutions, a potential scan rate of 1, 10 or 100 mV/s was employed on static or rotating disc specimens of area 0.25 cm^2. The rotation speed in the latter case was 4000 rpm.

2.4. Identification of nitrogen reactions

Cyclic voltammetry in 1 M H_2SO_4 + 1 M HCl and in 0.5 M NaCl was performed on static specimens between potential limits of −850 and +1150 mV SCE using potential scan rates of 10, 100 and 1000 mV/s. Polarisation curves were evaluated in synthetic pit solutions obtained by dissolving 25 g of steel in 100 ml 10 M HCl until saturation by holding for 2 days at 50°C, 2 days at 60°C and 6 h at 90°C, in accordance with the method of Hakkarainen [67]. A rotation speed of 1000 rpm was used to avoid salt film formation or concentration polarisation and the potential scan rate was 100 mV/s. Impedance measurements in HCl solutions were made on specimens of area 1 cm^2 which were polished to 0.5 μm alumina to reduces surface roughness effects. In most cases, the frequency range was 50 mHz to 10 kHz but, where necessary, the minimum frequency was reduced to 1 mHz. Quasi steady-state polarisation curves in the same environments were obtained by increasing the potential in steps of 10 mV and recording the current after 2 min at each potential. Solution analyses were performed after potentiostatic dissolution of specimens in various acidic chloride solutions using a combination of Kjeldahl or spectrophotometric analysis for HN_4^+ and flow injection analysis for $NO_3^- + NO_2^-$. The electrolyte volume was 20 ml and the exposed specimen area ranged between 1 cm^2 and 25 cm^2, depending on the dissolution current. Dissolution times of 6–150 h were used to achieve between 0.1 and 0.3 g of metal in solution.

3. Results

The critical temperatures for pitting corrosion in 0.2 M NaCl (Figure 1) increased linearly with nitrogen content over the range investigated The effect was more pro-

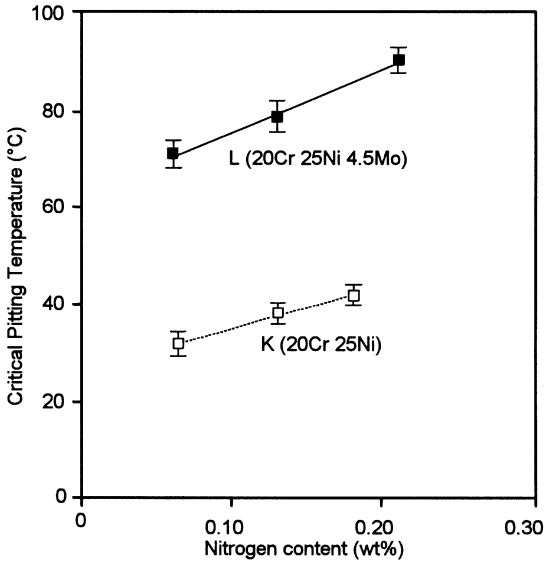

Fig. 1. Critical pitting temperature in 0.2 M NaCl at +600 mV SCE. Mo–N synergy is apparent from the steeper gradient for the L series with 4.5% Mo (144°C/%N) compared to the Mo-free K series (86°C/%N). Error bars denote maximum and minimum values.

nounced for the L series containing 4.5% Mo (CPT increase 144°C/%N) than for the Mo-free K series (CPT increase 86°C/%N). This indicates that there is a synergistic interaction between alloyed molybdenum and alloyed nitrogen in increasing pitting corrosion resistance, this has been treated quantitatively elsewhere [31].

Pit initiation sites (Figure 2) showed little dependence on alloy composition. The average pit diameter was approximately 5 μm but, in the majority of cases, their location could not be related to any particular microstructural feature. A few pits occurred on non-metallic inclusions, although the true figure may be somewhat higher due to dissolution or drop-out of inclusions during immersion in the $FeCl_3$–$AlCl_3$–glycerol–ethanol solution. The number of pits on grain boundaries corresponded closely to the theoretical value obtained from the grain size, average pit diameter and on assumption of random pitting. This observation, and the fact that all the alloys were single-phase austenitic steels free from precipitated secondary phases, excludes the possibility that microstructural modification could be responsible for the beneficial effects of alloyed nitrogen and molybdenum on pitting corrosion resistance. Microstructural effects of nitrogen are thus not an issue in these single-phase steels and are omitted from further discussion about possible nitrogen mechanisms.

The pitting potential measurements in Fig. 3 show the same trend of increasing pitting resistance with increasing nitrogen content, although the effect becomes less marked at higher testing temperatures. The necessity of using different temperatures for the K and L series prohibits specific evaluation of the effect of molybdenum or of Mo–N synergism. The lower lines in Fig. 3 show the potential at which current transients commence. These current transients are shown in the potentiodynamic

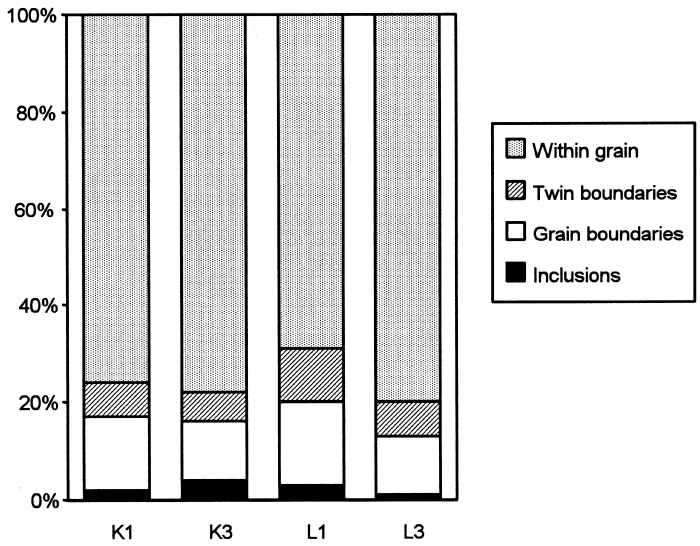

Fig. 2. Pit initiation sites in $FeCl_3+AlCl_3+$glycerol+ethanol at 20°C (K series) or 60°C (L series), determined for 300 pits per material. The number of pits on grain boundaries is close to the theoretical value calculated from the grain size.

curves for steels K0 and K3 in Fig. 4 together with the microstructures after testing, which demonstrate that these transients are associated with the initiation and repassivation of small pits. Nitrogen alloying produces a greater increase in the final pitting potential, E_b, than in the potential for initiation of repassivating pits, E_{init}, and thus broadens the potential range in which repassivating pitting occurs. This is comparable with the observation by Palit et al. [35] of metastable repassivating in nitrogen-alloyed steels at the same potential at which pitting occurred for low-nitrogen steels. The observations suggests that a primary role of nitrogen is in promoting pit repassivation rather than inhibiting pit initiation.

The passive currents in acidified 0.5 M NaCl showed a gradual decrease with time and plots (Figure 5) of $\log(i)$ vs. $\log(t)$ are linear over more than two decades, with gradients close to -1. This behaviour is consistent with film growth by high field ionic conduction [68] wherein the ionic current, i, through the film is related to the field, F, across the film by the relation, $i=\propto e^{\beta F}$. By manipulation, this yields the inverse logarithmic film growth law, $1/x=a-b\log t$, and it has been shown mathematically [69] that the gradient of $\log(i)$–$\log(t)$ varies from -0.87 to -0.96 as βF varies from 10 to 50, which should cover many real systems. This type of inverse logarithmic film growth has been observed by Stern [70] for 304 stainless steel passivating in ferric–ferrous sulphate solution and by Kirchheim et al. [71] for binary Fe–Cr alloys in H_2SO_4. Marshall and Burstein [72] also noted the same behaviour for ab initio passive film formation on scratched electrodes of 304. This passive current evolution indicates that the major part of the measured current is attributable to film thickening rather than to film dissolution, which would cause the curves to level off at lower current densities [71].

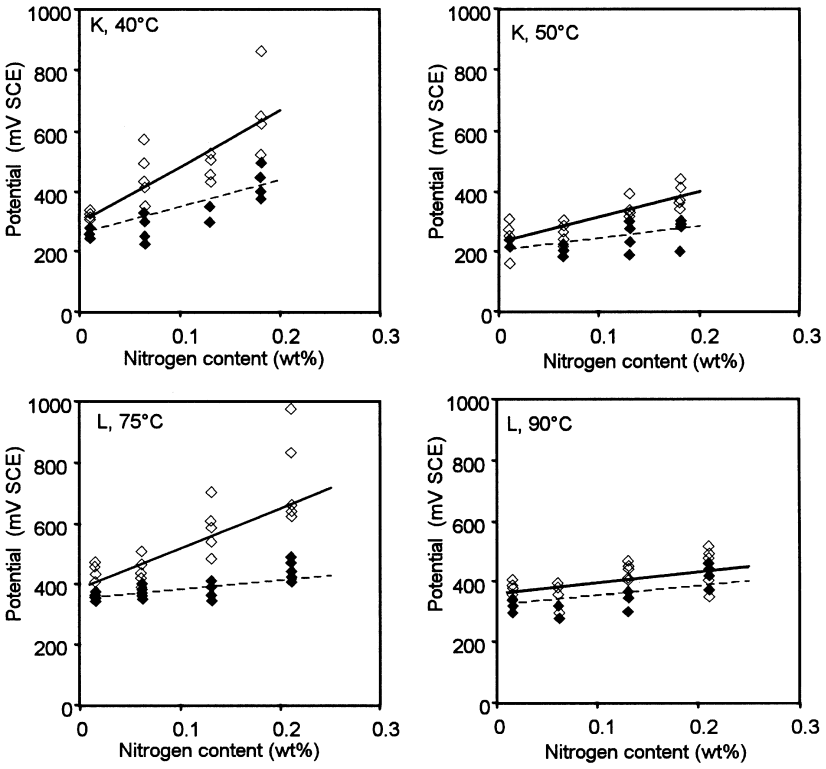

Fig. 3. Pitting potential measurements at various temperatures showing the final breakdown potential E_b (open points) and the potential E_{init} at which the first repassivating pits were observed (solid points).

The curves in Fig. 5 show that nitrogen decreases the passive current density, without affecting the gradient of the log(i)–log(t) plot so that, at a given time, less current is required for passive film growth on the nitrogen-bearing steels than on their low-nitrogen equivalents. The charge associated with passive film formation is thus reduced by nitrogen. An increase in potential from +150 to +600 mV SCE increased the passive current density but had little effect on the slope. On the other hand, molybdenum additions increased the gradient of the curves somewhat, from an average at +150 mV of −0.98 for the K series to −0.92 for the Mo-alloyed L series. The passive current densities were initially lower for the Mo-alloyed steels but they exceeded the values for the corresponding Mo-free steels at longer times.

Transient behaviour observed during the passive current density measurements is shown in Fig. 6. The transient currents were appreciably lower than those in Fig. 4 and there was no indication of pits or other surface attack on the specimens after testing, so these activations clearly represent a very early stage of passive film breakdown (sub-critical depassivation). Molybdenum reduced the number and magnitude of activations (compare L1 and K1). Nitrogen reduced the magnitude of the transients but had a variable effect on their number (reduced initially but increased at longer

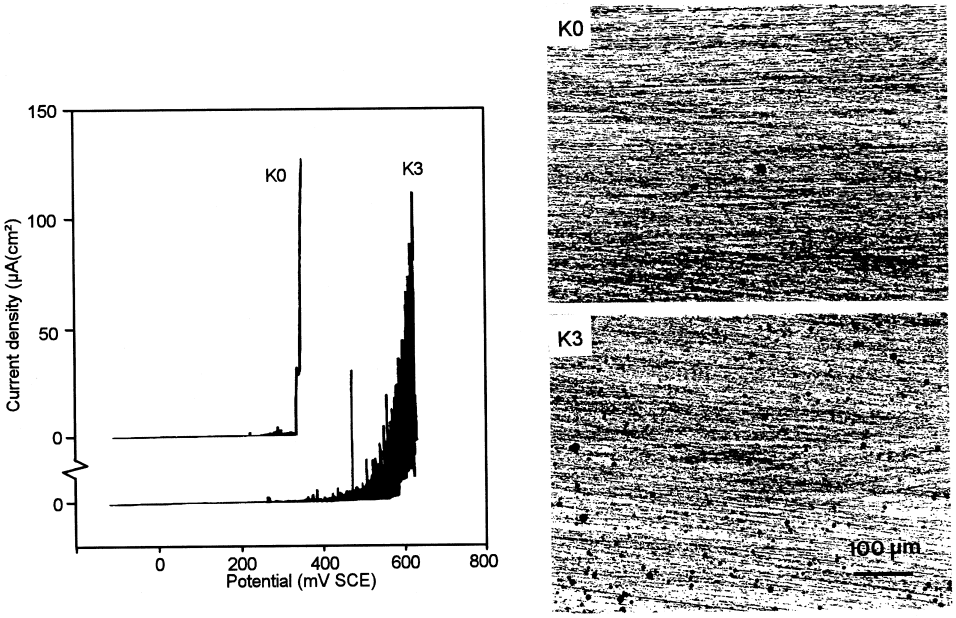

Fig. 4. Typical pitting potential measurements for K0 and K3 at 40°C. The first pits initated at similar potentials for both steels but repeated pit repassivation lead to a higher pitting potential for K3. The repassivated pits are visible on the specimen surface.

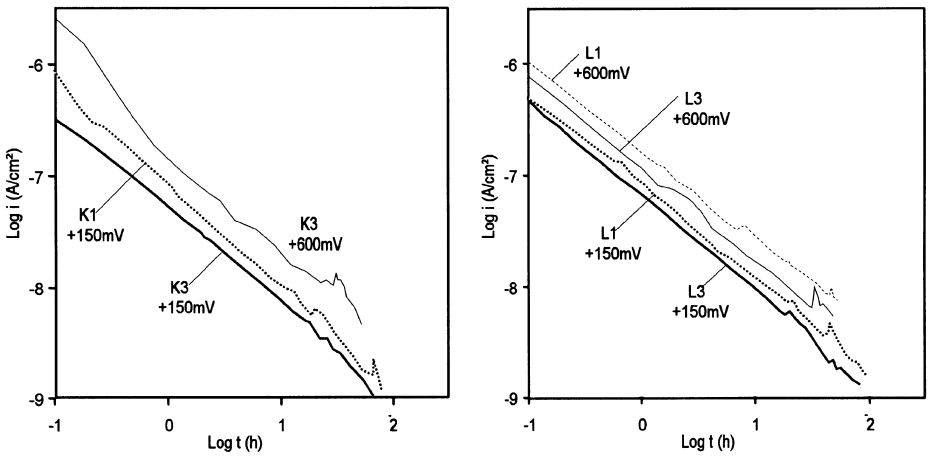

Fig. 5. Passive current densities measured in 0.5 M NaCl, pH = 3 at +600 mV SCE and +150 mV SCE. Passive current densities are decreased by nitrogen alloying, and the gradient is slightly increased by molybdenum. Steel K1 exhibited an irregularly increasing current density at +600 mV SCE.

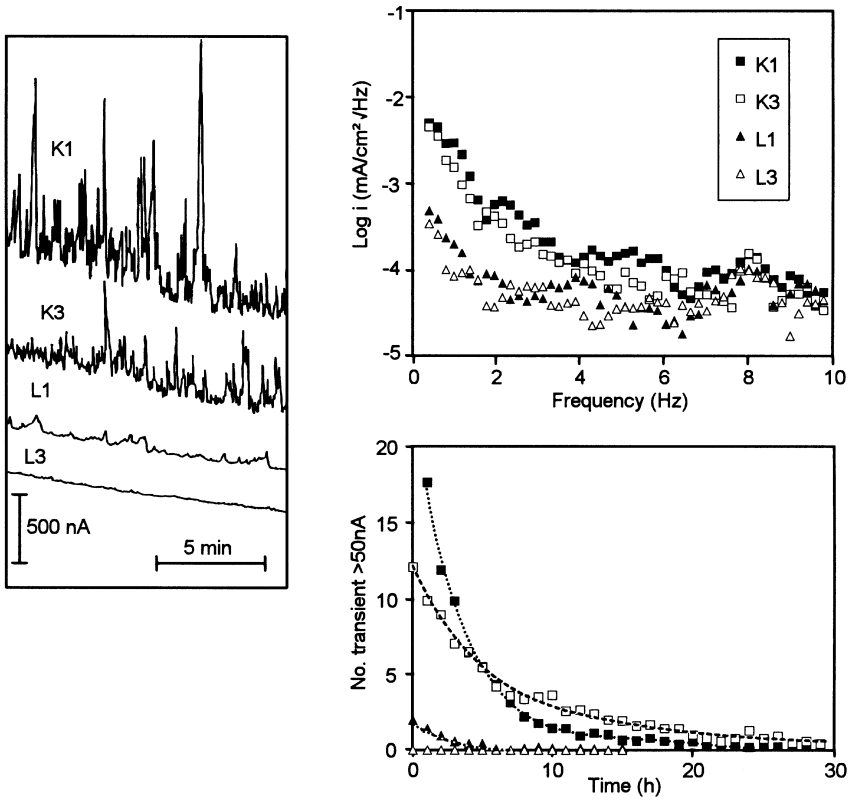

Fig. 6. Current transients measured during passive current density measurements in 0.5 M NaCl, pH 3 at +150 mV SCE. (a) Current–time trace after 30 min. (b) Current noise after same time. (c) Number of activations (>50 nA).

times in 0.5 M NaCl at pH 3 and +150 mV SCE, vice versa in 0.9 M NaCl +0.1 M HCl at the same potential). A reasonable interpretation of this behaviour is that molybdenum increases resistance to depassivation while the primary role of nitrogen is in promoting repassivation. The elimination of activations (>50 nA) for L3 with 4.5% Mo and 0.21% N demonstrates the synergistic interaction between these two alloying elements. Transients at +600 mV SCE were very similar to those at +150 mV SCE. No activations were observed for L3 even at this higher potential so the possibility that transients only reflected the proximity of the pitting potential can be excluded.

The peak anodic current density obtained in polarisation curves in HCl of various concentrations (Figure 7) showed that molybdenum appreciably decreased the dissolution rate over the entire HCl concentration range investigated. The effect of nitrogen was most marked in the intermediate concentration range, as previously observed by Newman and Shahrabi [2]. Reversal of the potential sweep direction immediately after passing the current peak was used to investigate the wider validity

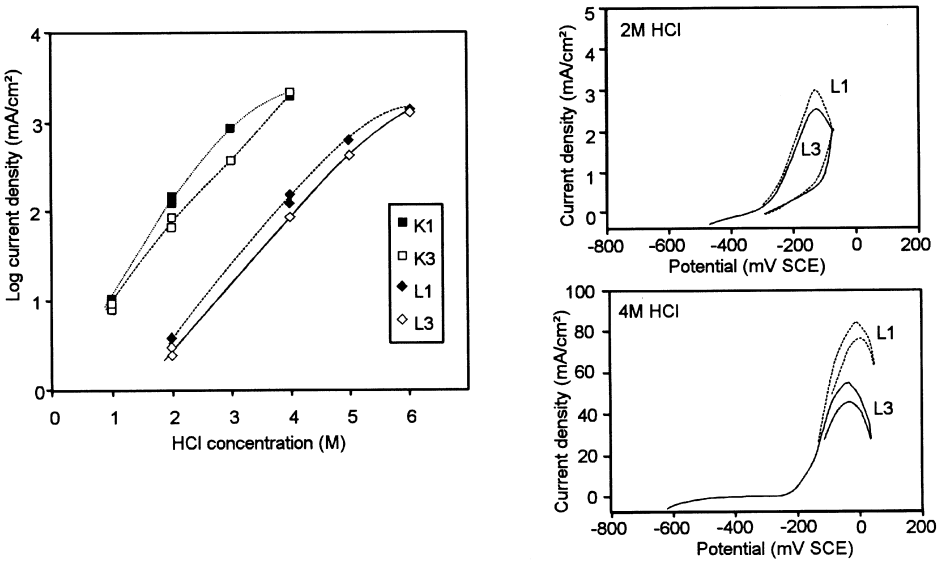

Fig. 7. (a) Peak anodic current density in HCl at 10 mV/s The effect of nitrogen in decreasing the peak anodic current density is most pronounced at intermediate HCl concentrations. (b) Effect of potential scan reversal on polarisation curves. In 2 M HCl, passivation proceeds when the potential is decreased; in 4 M HCl, the passivation process is reversed for both L1 and L3.

of their hypothesis that a reversible current peak was characteristic for nitrogen-alloyed steels and indicative of quasi-passivation caused by nitrogen accumulation at surface step sites. Reversal of the polarisation direction in 2 M HCl led to a continuation of the passivation process for both N-bearing and N-free steels while, in 4 M HCl, the passivation process exhibited reversibility in both cases [Fig. 7(b)]. There was thus no indication that the passivation process was different in the presence of alloyed nitrogen and it appears that passivation by oxide film formation may satisfactorily explain the observed behaviour for both high- and low-nitrogen steels in the present investigation.

RDE investigations showed no systematic effect of solution transport on the peak anodic current density in any of the HCl solutions investigated, as illustrated in Fig. 8 for L1 and L3 in 4 M HCl. This indicates that salt film precipitation conditions have not been reached in any instance. The similarity between the stationary experiments and those at 4000 rpm also shows that any effect of nitrogen is occurring within the hydrodynamic boundary layer (in this case 180 μm from the surface).

Polarisation curves in 1 M H_2SO_4 with various additions of HCl [Fig. 9(a)] demonstrated that the effect of nitrogen on the dissolution rate (maximum anodic current density) is not unequivocally beneficial. For the K series the maximum current density in 1 M H_2SO_4 + 1 M HCl was reduced by nitrogen alloying but a shift to the reverse trend occurred with decreasing HCl additions. In the Mo-alloyed L series the beneficial effect of nitrogen was retained even down to 0.2 M HCl, again suggesting the occurrence of Mo–N interaction. The entire polarisation curves [Fig. 9(b,c)] show that the

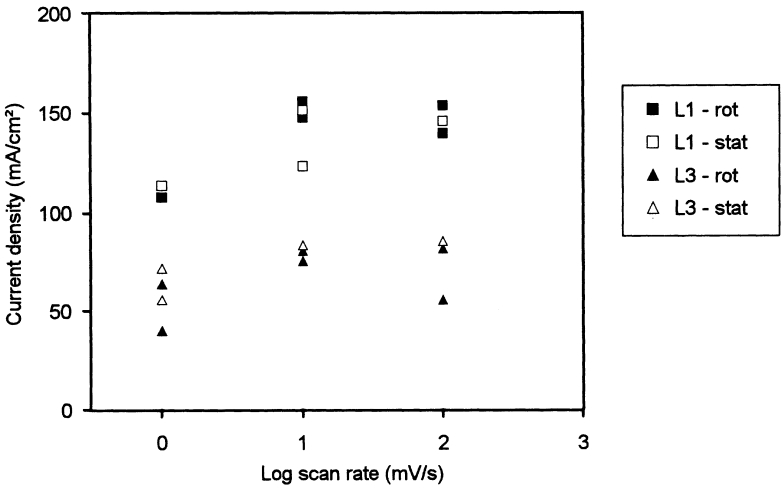

Fig. 8. Peak anodic current density for L1 and L3 in 4 M HCl at various potential scan rates and rotation speeds. 'rot' denotes 4000 rpm.

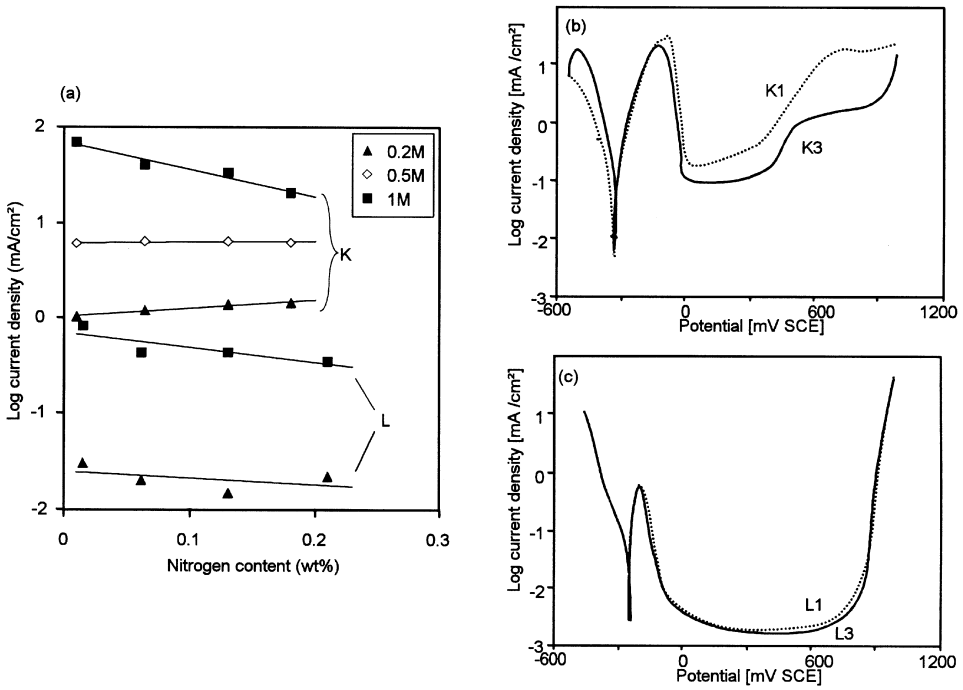

Fig. 9. (a) Peak anodic current densities, at a potential scan rate of 20 mV/min, in 1 M H_2SO_4 with additions of 0.2–1 M HCl showing the variable effect of nitrogen alloying. (b) and (c) Polarisation curves in 1 M H_2SO_4 + 1 M HCl.

passivation potential and passive current densities in 1 M H_2SO_4 + 1 M HCl were slightly reduced by nitrogen. These two effects were retained even at lower HCl concentrations.

Impedance measurements were made in 1 M HCl, 1 M HCl + 3 M NaCl, 2 M HCl + 2 M NaCl and 4 M HCl. Up to four different arcs were apparent from the complex-plane plots (Figs. 10, 11) and results were analysed in terms of an equivalent circuit, comprising a hierarchical arrangement of four stacked resistor–capacitance pairs. In parallel to a previous analysis [73], arc a1 is interpreted as reflecting the double layer capacitance ($C1$) and charge transfer resistance ($R1$), and arc a2 as an adsorbed reaction intermediate, probably iron. Arc a3 is related to the passivation process since $R3$ tended to infinity at the current maximum and, thereafter, became negative. The lowest-frequency arc, a4, was most clearly visible for the L series in the concentrated electrolytes but was frequently obscured by data scatter at low frequencies, particularly at higher potentials, so its interpretation is uncertain. The

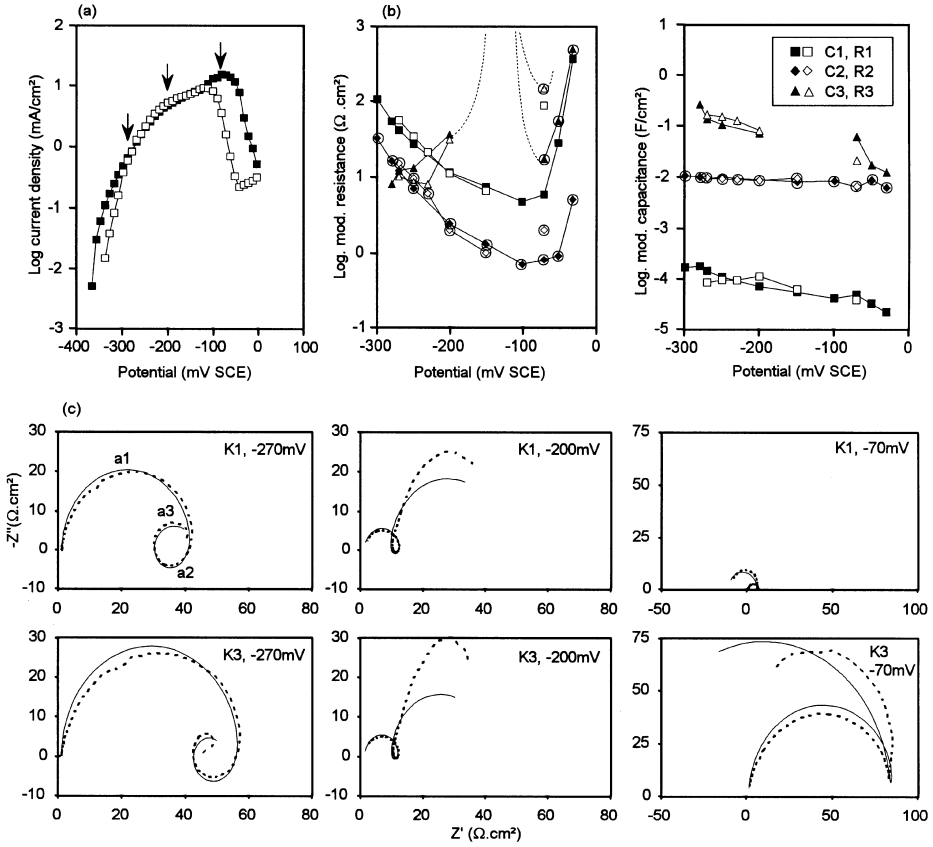

Fig. 10. EIS measurements in 1 M HCl. (a) Quasi steady-state polarisation curves. (b) Evaluated impedance parameters for K1 and K3. Circled points are negative, solid points are for K1 and open points for K3. (c) Typical complex-plane plots showing experimental points and fitted curves.

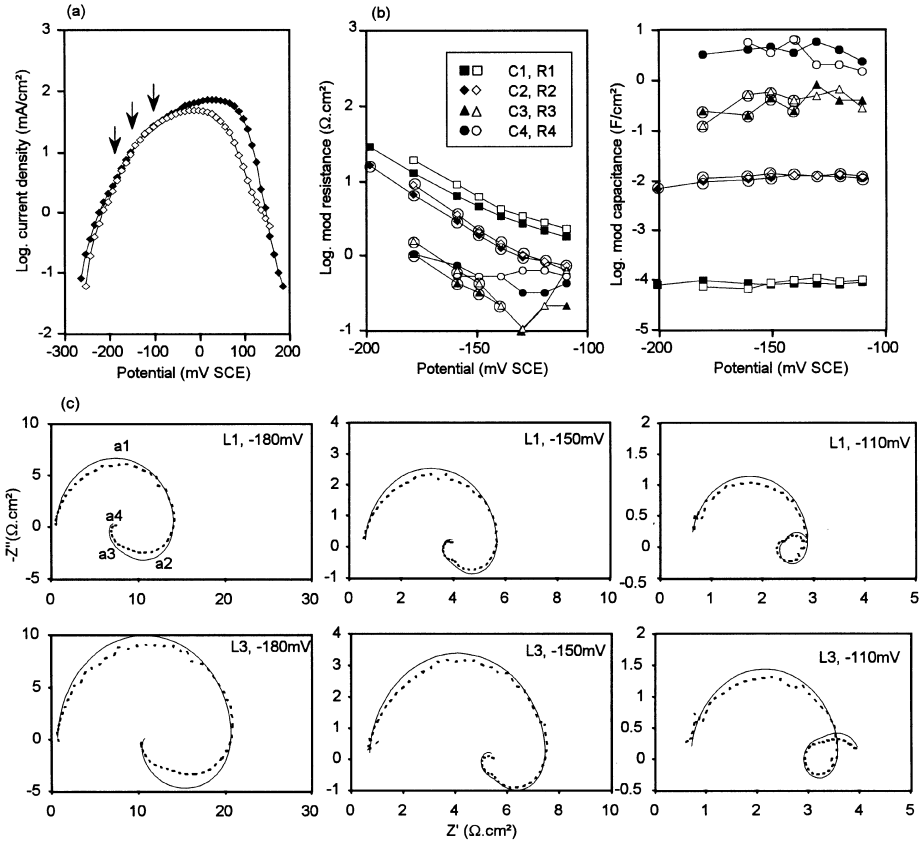

Fig. 11. EIS measurements in 4 M HCl. (a) Quasi steady-state polarisation curves. (b) Evaluated impedance parameters for L1 and L3. Circled points are negative, solid points are for L1 and open points for L3. No values could be obtained at higher potentials due to large data scatter at high current densities. (c) Typical complex-plane plots showing experimental points and fitted curves.

effect of nitrogen on the evaluated impedance parameters was small and could be accounted for by the earlier onset of passivation in the nitrogen-bearing steels. There was no indication of any additional time constant or other characteristic behaviour in the impedance response which could be related to the presence of nitrogen in the alloy. In the case of molybdenum alloying, appreciable effects were observed and have been treated in detail elsewhere [73].

Cyclic voltammetry in 1 M H_2SO_4 + 1 M HCl and in 0.5 M NaCl gave no indications of nitrogen reactions. Solution analyses (Fig. 12) after dissolution of the K and L series steels in a wide range of environments demonstrated that, in all cases, the majority of the nitrogen dissolving from the steel was present as ammonium ions (NH_4^+) in solution. This was even the case when dissolution occurred in a potential-pH region in which NO_3^- is the thermodynamically stable nitrogen species, suggesting that the kinetics of nitrogen reactions are slow. In only five of twenty cases did the

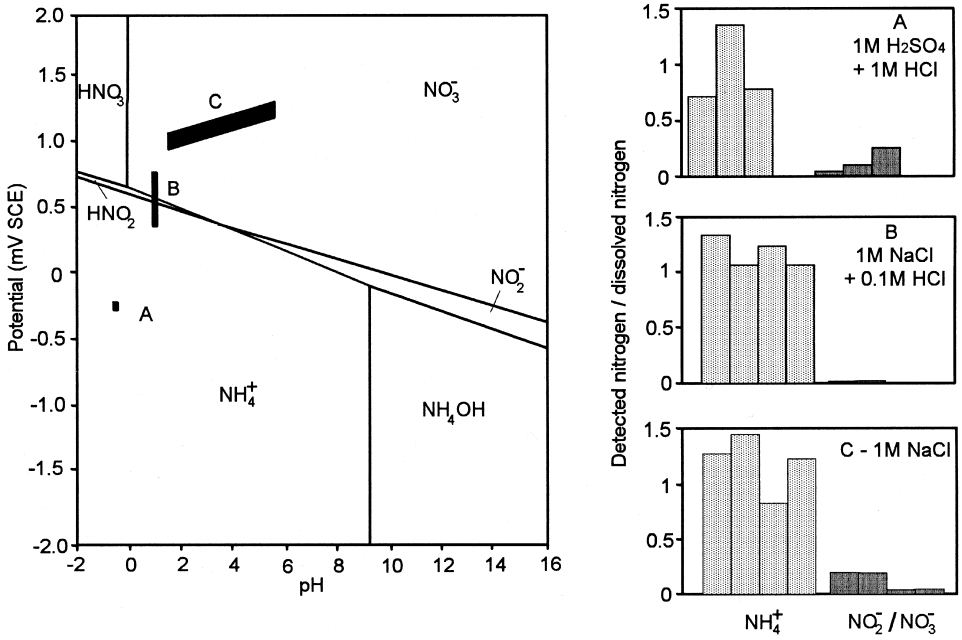

Fig. 12. Pourbaix diagram [74] for nitrogen showing potential–pH regions in which solution analyses were performed for K3 and proportion of the dissolved nitrogen (from weight loss measurements) analysed as NH_4^+ or NO_2^-/NO_3^-. Dissolution was by active corrosion in A, pitting corrosion in B and transpassive corrosion in C.

amount of $NO_3^- + NO_2^-$ exceed 5% of the dissolved nitrogen, four of these cases are included in Fig. 12. These results are in agreement with those of Osozawa and Okato [7, 8] who found NH_4^+ to dominate after dissolution in 20% $FeCl_3$, which is also an acidic chloride with a high redox potential.

In order to investigate the possible role of dissolution products, synthetic pit solutions were prepared by dissolving various steels in 10 M HCl. The final pH of the solutions differed somewhat, being 0.18 for K1-solution, 0.36 for K3-solution, 0.52 for L1-solution and 0.27 for L3-solution. There was no discernible effect of alloyed nitrogen on the polarisation behaviour, so the polarisation curves are typified by the curves for steels K1 and L1 in Fig. 13. K1 and K3 showed no evidence of passivation and exhibited current densities of over 200 mA/cm^2 at +600 mV SCE; the corresponding current densities on L1 and L3 were below 5 mA/cm^2. The anodic current density was largely unaffected by solution species, while the cathodic current density reflected the solution pH (higher for K1 solution than K3, higher for L3 solution than L1). The latter was confirmed by HCl additions to some of the solutions. As was reported by Hakkarainen [67], molybdenum in the alloy was found to shift the dissolution range to more noble values. However, in contrast to the negligible effect of solution molybdenum observed by Hakkarainen, molybdenum in solution in this study was found to cause an appreciable drop in the corrosion potential, indicating the presence of a readily-reduced species.

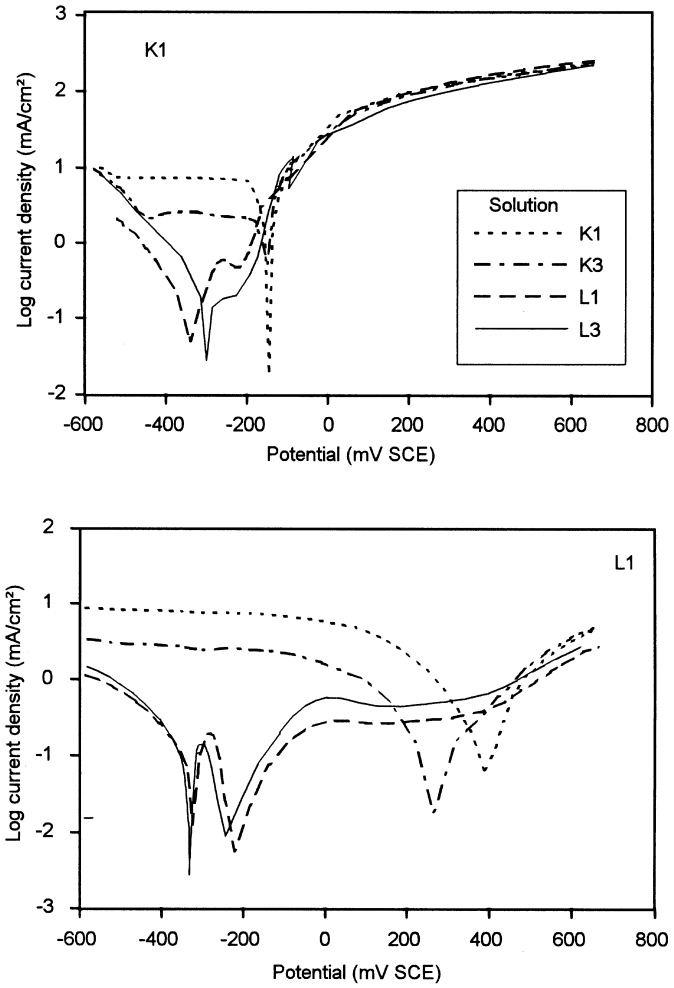

Fig. 13. Polarisation curves for K1 and L1 at 100 mV/s and 1000 rpm in synthetic pit solutions obtained by dissolving steels in 10 M HCl. Nitrogen in solution has no significant effect, the presence of dissolved molybdenum reduced the corrosion potential.

4. Discussion

The basic effects observed for the 20 Cr–25 Ni (4.5 Mo) steels investigated here are that nitrogen increases pitting corrosion resistance, and depresses both active dissolution and passive current densities. These findings are in agreement with the majority of reported investigations and define the basic framework which must be covered by any proposed mechanism for the nitrogen effect. In addition, there are two further effects which are apparent in several of the investigations performed here and which per se provide mechanistically useful information. The first is that nitrogen

enhances *repassivation*. This is apparent in the pitting potential measurements, in that the potential for the initiation of the first pits is similar for both low- and high-nitrogen steels but repeated repassivation of pits in the latter case leads to a higher final breakdown potential. Similarly, nitrogen also reduces the magnitude of the subcritical depassivation events, apparent as transients during passive current density measurements. The second major effect is that of *Mo–N synergism*. This is apparent in the CPT results, also in the passive current density measurements and the polarisation curves in acidic solution. During the passive current density measurements, molybdenum appreciably reduces the number of depassivation events, as evidenced by current transients, while Mo and N in combination effectively eliminate these transients. Polarisation curves also show that the beneficial effect of nitrogen in reducing active dissolution is retained to lower critical current densities in the presence of molybdenum.

4.1. Solution chemistry

On the basis of thermodynamics [74], ammonium is the stable species at low potentials and pH (such as occur in pits and crevices) but nitrate should dominate at high potentials. However, the solution analyses after dissolution under active, pitting and transpassive dissolution conditions Fig. 12 demonstrate unequivocally that NH_4^+ is the dominant dissolution product of the nitrogen in solid solution in the steel. This indicates that reaction kinetics rather than thermodynamics are of overriding importance in the electrochemistry of nitrogen dissolution. However, it does not provide any indication of the surface reaction taking place. Equations (1, 2 and 5) all result in NH_3/NH_4^+ formation, but make different assumptions about the state of the surface nitrogen prior to dissolution. Equation (1) is cathodic and thus should slow down as the potential is raised. In contrast, eq. (2) and eq. (5) are potential independent in that they involve a reduced form of nitrogen (nitride or N^{3-}) on the surface, and are thus more probable candidates for ammonium formation under a wide range of conditions. This aspect is discussed further in Section 4.2, on surface segregation, below.

This dominant presence of NH_4^+ after dissolution effectively excludes a nitrate-based mechanism. At high potentials, a nitrate mechanism would require that the thermodynamically stable NO_3^- be reduced to the NH_4^+ which is detected. A mechanism whereby NH_4^+ is formed initially and then oxidised to NO_3^- with an inhibiting function (see Section 1.4) is likewise excluded as this would require the process $NH_4^+ \rightarrow NO_3^- \rightarrow NH_4^+$ to occur. Further convincing evidence that NH_4^+ is the critical species has been supplied by the elegant work of Kim et al. [75]. They exposed pure Cr in nitrate-containing solutions at various potentials and demonstrated with XPS that nitrate was reduced to NH_3/NH_4^+ over the potential range from -930 to $+1300$ mV SCE, also that reduction to a surface nitride could occur when the passive film was absent (at low potential) or damaged (high potential). This again contradicts the thermodynamic data and again indicates that nitrogen in stainless steels does not oxidise to NO_3^-.

The second question with regard to solution chemistry is whether the NH_4^+ for-

mation has a sufficient effect on surface pH to facilitate repassivation. Pawel et al. [16] have raised objections to the NH_4^+ theory on the grounds that the pH effect is unlikely to be sufficient in strongly acidic solutions, while Bandy et al. [10] have pointed out that both Mo and N form a variety of products but that these may have nothing to do with the primary inhibiting mechanism.

An order of magnitude calculation may be performed using typical hydrolysis reactions [64, 4]:

$$Fe + 2H_2O \rightarrow FeOOH^- + 3H^+ + 2e^-, \quad (6)$$

$$Cr + 4H_2O \rightarrow CrO_4^{2-} + 8H^+ + 6e^-, \quad (7)$$

$$Mo + 4H_2O \rightarrow MoO_4^{2-} + 8H^+ + 6e^-. \quad (8)$$

Assuming retention of all dissolution products within a pit, nitrogen dissolution as NH_4^+ according to eq. (1) would, for steel L3 compared to L1, mitigate the pH drop due to hydrolysis by less than 1%. However, it should be noted that cation chloride complexing will significantly reduce the acidifying effect of metal dissolution and thereby increase the relative importance of NH_4^+ in buffering the pH. Evidence that the pH effect is measurable is provided by the study of Azuma et al. [44] who galvanostatically dissolved a 25 Cr–25 Ni–10 Mn steel in deaerated 5% NaCl and found that, after 20 h dissolution, the pH within a small anolyte volume had fallen to $\sim$2.1 in the N-free steel but only $\sim$2.3 with 0.364% N. A further argument in this context is that NH_4^+ formation is a surface reaction. H^+ scavenging by dissolving nitrogen may therefore have a profound effect in the near-surface solution which is otherwise dominated by contact adsorption of OH^- and Cl^- on the metal surface.

Two further aspects of solution chemistry are illuminated by the results of the present study. The first is that the polarisation curves in synthetic pit solution show that the presence of ammonium in solution does not per se have a significant influence on polarisation characteristics. This eliminates any idea of an inhibiting effect of this species. The second point is that rotating disc studies demonstrate conclusively that the effect of nitrogen occurs within the hydrodynamic layer (180 μm), again excluding the idea of a significant bulk solution modification.

4.2. Surface segregation

One question in terms of surface segregation which is open to critical evaluation is the suggestion by Newman and Shahrabi [2], detailed in Section 1.7, that anodic segregation of nitrogen may block surface dissolution sites and thereby cause quasi-passivation. Information in this context is provided by the electrochemical behaviour in acidic chloride solutions. These environments are of particular interest because they approximate to conditions prevailing during propagating pitting or crevice corrosion. At all the concentrations investigated here, 0.2 to 6 M HCl, there was no evidence of salt film formation prior to passivation. This is in notable contrast to the work of the aforementioned authors [2] in which borderline conditions were identified

where a 17 Cr–12 Ni–2.5 Mo steel exhibited salt film formation, but the corresponding alloy with 0.22% N exhibited reversible passivation.

In the present investigation, the passivation process was found to be the same for both low and high nitrogen steels. In less aggressive environments, passivation proceeded when the potential sweep direction was reversed from the anodic to the cathodic direction just after passing the active dissolution peak while, in more concentrated HCl solutions, reversible passivation occurred Fig. 7. Although reversible passivation may, in some cases, be attributable to surface nitrogen accumulation, as suggested by Newman and Shahrabi [2], this is clearly not the case in the alloy systems investigated here. The observed effects are instead consistent with conventional passivation by oxide film formation. A second observation which argues against the hypothesis that sluggish nitrogen dissolution causes kink site blockage due to nitrogen accumulation is that of impedance measurements. There is no indication in the impedance measurements of any additional time constant which can be related to the presence of nitrogen in the steel. Thus there is no support for the idea that eq. (1) has become the rate determining step for dissolution of the entire alloy. On the contrary, it appears that nitrogen only causes slight modification of the impedance parameters relating to dissolution of other alloy components and to passive film formation. However, the impedance results do not exclude the possibility of surface nitrogen bonding which limits dissolution of all species.

The issue of whether surface segregation is occurring to any extent is more difficult to treat on the basis of electrochemical measurements alone. However, at least one observation in the present study cannot be readily explained only by solution chemistry effects, namely that nitrogen decreased the passive current density so less charge was requires for passive film formation. A parallel may be drawn to the effect of increasing levels of Cr on the passive current density for Fe–Cr alloys [71]. Whether this effect of nitrogen is attributable to a decrease in film thickness or to an alteration in film/surface properties cannot be ascertained from the available data, but it is clearly not related to ammonium formation in that a negligible amount of dissolution is taking place. A possible explanation is provided by the concept of surface nitrogen accumulation. Ample evidence for nitrogen enrichment beneath the passive film has been supplied by surface analytical investigations, as detailed in Section 1.6, and such an effect may well explain the present results. Molybdenum alloying appears to have a different effect on passive film growth since it decreases the gradient of the $\log(i)$–$\log(t)$ plots in Fig. 5. As discussed by Kirchheim [76], this may be due to a larger amount of dissolution occurring during passive film formation or to changes in diffusivity within the film. The specific observation of Marshall and Burstein [77] that molybdenum raises the electric field over the film and thereby promotes dissolution of the iron component during the early stages of film formation on scratched electrodes, may also be of relevance, even though the increased charge that they observed to be associated with passivation in molybdenum-alloyed steels is not apparent at the longer times investigated here.

If, on the basis of the convincing body of evidence in the literature, it is accepted that surface segregation of nitrogen does occur to some extent, then several forms of nitrogen are possible. Segregated atomic nitrogen, negatively charged nitrogen and a

nitride phase have variously been suggested. The interfacial compositions evaluated by Olefjord and Wegrelius [47], using variable angle XPS, correspond to a nitrogen content in the subfilm monolayer of 3–6 wt.%, the corresponding value from the AES investigation of Lu et al. [56] is 3%. These values are within the range of typical nitrogen contents in nitrides (e.g. 12% in Cr_2N, 5% in η phase, 1.5% in π-phase [78]) so nitride bonding (or at least a negatively charged nitrogen species) appears more probable than either atomic nitrogen enrichment in solid solution or surface intermetallic phase formation. Much of the XPS evidence detailed in Section 1 also points to negatively charged surface nitrogen species. Obviously, no evidence for the form of surface segregated nitrogen can be provided by the present electrochemical investigation, but it can be pointed out that the presence of a reduced form of nitrogen in the metallic state is more compatible with the observed ammonium formation, since the latter can then be attributed to eq. (2) or eq. (5). Equation (1), in contrast, is a cathodic reaction and thus difficult to reconcile with observations of ammonium at high potentials.

Another interesting effect of mechanistic significance in this context is the range over which nitrogen affects the critical current density. For the Mo-free K series of steels, a beneficial effect of nitrogen on active dissolution is just apparent in 1 M $H_2SO_4 + 0.5$ M HCl, in which the critical current densities are around 10 mA/cm^2 while, at a lower HCl concentration, a slight detrimental effect is observed instead. In contrast, for the Mo-alloyed L series of steels, the beneficial effect is still apparent in 1 M $H_2SO_4 + 0.2$ M HCl at critical current densities just above 10 μA/cm^2. These current densities correspond to charges of 3 C/cm^2 and 3 mC/cm^2 and thus the dissolution of approximately 5000 and 5 atomic layers respectively. One possible explanation of this behaviour is that molybdenum enhances surface retention of nitrogen. For both Cr–Ni and Cr–Ni–Mo steels, the beneficial effect of nitrogen on active dissolution disappears in more aggressive solutions, at critical current densities of the order of 1 A/cm^2. It may be that the NH_4^+ effect is insufficient to buffer even the near-surface pH if the solution becomes sufficiently aggressive, but this effect may also be related to surface segregation and interaction.

In summary, although a number of proposed mechanisms for the effect of nitrogen on corrosion resistance can be excluded as explanations for the effects observed in the present study, there are several mechanisms that appear to be relevant and are probably acting simultaneously. Surface nitrogen accumulation and an altered surface bonding state, possibly approximating to nitride formation, are important. pH buffering by NH_4^+ formation, probably from a nitride or negatively charged nitrogen state, as described in eq. (2) or eq. (5), is also of significance. However, the relative importance of the effects is still an open question and may depend on the specific dissolution condition under investigation.

5. Conclusions

1. Additions of nitrogen to 20 Cr–25 Ni (4.5 Mo) austenitic stainless steels improve pitting corrosion resistance, particularly in the presence of molybdenum. The

dominant effect of nitrogen is associated with repassivation, while molybdenum appears to act at an earlier stage and suppress initiation. Pit initiation sites are not affected by alloying with nitrogen or molybdenum.
2. Nitrogen alloying reduces active dissolution in acidic chloride solutions and is most efficient at intermediate dissolution rates. The effect is apparent to lower critical current densities in the molybdenum-alloyed steels.
3. No salt film formation occurred and electrochemical passivation characteristics are identical for low- and high-nitrogen steels.
4. Ammonium ions are the dominant nitrogen species obtained when nitrogen-bearing steels are dissolved in active dissolution, pitting and transpassive conditions. The predominance of NO_3^-, predicted on thermodynamic grounds at high potentials, is not observed, indicating that reaction kinetics are of overriding importance.
5. Impedance measurements provide no evidence that anodic segregation of nitrogen causes a fundamental shift in the passivation process, nor that slow nitrogen dissolution is the rate determining step.
6. Nitrogen decreases the passive current density while molybdenum alters film growth characteristics. The effect of nitrogen is most readily attributable to nitrogen accumulation beneath the passive film.
7. Both surface accumulation of nitrogen and pH buffering by NH_4^+ formation are probably operative mechanisms which can explain the beneficial influence of nitrogen on various aspects of corrosion resistance. The relative importance of the two effects may vary depending on the dissolution conditions.

Acknowledgements

The financial support for this work by Avesta Sheffield AB, AB Sandvik Steel, Avesta Sandvik Tube AB, Fagersta Stainless AB and the Swedish Board for Industrial and Technical Development (NUTEK) is gratefully acknowledged. Thanks are also expressed to Avesta Sheffield AB and AB Sandvik Steel for preparation of the laboratory heats, and to SRI International for provision of facilities for conducting the EIS measurements.

References

[1] C.R. Clayton, K.G. Martin, in: Proc. Conf. High Nitrogen Steels, 1988, pp. 256–260.
[2] R.C. Newman, T. Shahrabi, Corrosion Science 27 (8) (1987) 827–838.
[3] P.R. Levey, A. van Bennekom, Corrosion 51 (12) (1995) 911–921.
[4] H.J. Grabke, ISIJ International 36 (7) (1996) 777–786.
[5] M.O. Speidel, in: Proc Int. Conf. Stainless Steels, Chiba, 1991, pp. 25–35.
[6] M. Janik-Czachor, E. Lunarska, Z. Szklarska-Smialowska, Corrosion 31 (11) (1975) 394–398.
[7] K. Osozawa, N. Okato, Y. Fukase, K. Yokota, in: 5th Int. Conf. Metallic Corrosion, 1972, pp. 270–274.
[8] K. Osozawa, N. Okato, in: Proc. USA–Japan Seminar: Passivity and its Breakdown on Iron and Iron-Based Alloys, Honolulu. NACE, 1976, pp. 135–139.

[9] J.E. Truman, M.J. Coleman, K.R. Pirt, British Corrosion Journal 12 (4) (1977) 236–238.
[10] R. Bandy, Y.C. Lu, R.C. Newman, C.R. Clayton, Proc Electrochemical Society 84 (9) (1984) 471–481.
[11] C.R. Clayton, L. Rosenzweig, M. Oversluizen, Y.C. Lu, Proc. Electrochemical Society 86 (7) (1986) 323–339.
[12] G.P. Halada, C.R. Claton, D. Kim, J.R. Kearns, Paper No. 531. in: NACE/Corrosion 1995.
[13] Sh. Song, W. Song, Zh. Fang, Corrosion Science 31 (1990) 395–400.
[14] R. Bandy, D. Van Rooyen, Corrosion 39 (6) (1983) 227–236.
[15] J.J. Eckenrod, C.W. Kovach, ASTM STP 697. 1979, p. 17.
[16] S.J. Pawel, E.E. Stansbury, C.D. Lundin, Corrosion 45 (2) (1989) 125–133.
[17] T. Tsuge, Y. Tarutani, T. Kudo, Paper 156. in: NACE/Corrosion '86.
[18] S. Hertzman, E. Symniotis, in: Proc. Stainless Steels '91, Chiba, 1991, pp. 1085–1092.
[19] U. Kamachi Mudali, R.K. Dayal, T.P.S. Gill, J.B. Gnanamoorthy, Werkstoffe u. Korrosion 37 (1986) 637–643.
[20] H.J. Grabke, S. Hirsch, B. Reynders, M. Stratmann, S. Tomec, in: Proc. High Nitrogen Steels, Kiev, 1993, pp. 513–517.
[21] R.F.A. Jargelius-Pettersson, A. Johansson, P. Gustafson, A. Sjöberg, S. Hertzman, L. Arnberg, R. Lagneborg, in: International Conference on High Nitrogen Steels, Aachen, 1990.
[22] S.D. Chyou, H.C. Shih, Materials Science and Engineering A129 (1990) 109–117.
[23] M.A. Streicher, J. Electrochemical Society 103 (7) (1956) 375–390.
[24] H.J. Dundas, A.P. Bond, Paper No. 159. in: Corrosion '75, NACE, 1975.
[25] G. Herbsleb, K.-J. Westerfeld, Werkstoffe und Korrosion 27 (7) (1976) 479–486.
[26] K. Shiobara, J. Japan Inst Metals 42 (9) (1978) 916–922.
[27] R.C. Newman, Y.C. Lu, R. Bandy, C.R. Clayton. in: Proc 9th Int. Conf. Metallic Corrosion, Toronto, vol. 3, 1984, pp. 394–399.
[28] Y.C. Lu, M.B. Ives, Corrosion Science 33 (2) (1992) 317–320.
[29] Y.C. Lu, M.B. Ives, C.R. Clayton, Corrosion Science 35 (1-4) (1993) 89–96.
[30] R.F.A. Jargelius-Pettersson, T. Wallin, in: Proc. 10th Scandinavian Corrosion Congress, 1986.
[31] R.F.A. Jargelius-Pettersson, Corrosion 54 (2) (1998) 162–168.
[32] A. Sadough Vanini, R. Chikhi, P. Marcus, Bulletin du Cercle d'Etudes des Métaux 16 (10) (1995) 6.3.
[33] K. Zagorski, A. Doraczynska, Corrosion Science 16 (1976) 405–410.
[34] H. Ezuber, A.J. Betts, R.C. Newman, Materials Science Forum 44/45 (1989) 247–258.
[35] G.C. Palit, V. Kain, H.S. Gadiyar, Corrosion 49 (12) (1993) 977–991.
[36] A. Sadough Vanini, J.P. Audouard, P. Marcus, Corrosion Science 36 (11) (1994) 1825–1834.
[37] U. Kamachi Mudali, B. Reynders, M. Stratmann, in: 7th Int. Symp. Passivity of Metals and Semiconductors, Clausthal, 1994.
[38] Y.C. Lu, M.B. Ives, Bulletin du Cercle d'Etudes des Metaux 16 (1) (1991) 16.1–16.6.
[39] G.P. Chernova, L.A. Chigirinskaya, N. Tomashov, Protection of Metals 16 (1) (1980) 1–5.
[40] R.F.A. Jargelius-Pettersson, in: Proc Eurocorr '92, 1992, pp. 119–128.
[41] R.F.A. Jargelius-Pettersson, ISIJ International 36 (7) (1996) 818–824.
[42] R.F.A. Jargelius-Pettersson, S. Hertzman, P. Szakalos, P.J. Ferreira, in: Proc. 4th Int. Conf. Duplex Stainless Steels, Glasgow, 1994.
[43] Ya.M. Kolotyrkin, I.A. Stepanov, V.M. Knyazheva, S.G. Babich, in: 9th Int. Conf. Metallic Corrosion, Toronto, vol. 1, 1984, pp. 258–263.
[44] S. Azuma, H. Miyuki, T. Kudo, ISIJ International 36 (7) (1996) 793–798.
[45] W.T. Tsai, B. Reynders, M. Stratmann, H.J. Grabke, Corrosion Science 34 (1993) 1647.
[46] C.-O.A. Olsson, Corrosion Science 37 (3) (1995) 467–479.
[47] I. Olefjord, L. Wegrelius, Corrosion Science 38 (7) (1996) 1203–1220.
[48] I. Olefjord, C.R. Clayton, ISIJ International 31 (2) (1991) 134–141.
[49] E. McCafferty, P.M. Natishan, G.K. Hubler, Corrosion 53 (7) (1997) 556–561.
[50] R.D. Willenbruch, C.R. Clayton, M. Oversluizen, D. Kim, Y. Lu, Corrosion Science 31 (1990) 179–190.
[51] G.P. Halada, D. Kim, C.R. Clayton, Corrosion 52 (1) (1996) 36–46.
[52] R. Bandy, D. Van Rooyen, Corrosion 41 (4) (1985) 228–233.

[53] J.E. Truman, in: Proc. UK Corrosion, Brighton, 1987, pp. 111–128.
[54] J.R, Galvele, in: R.P. Frankenthal, J. Kruger (Eds.), Passivity of Metals. The Electrochemical Society, 1978, p. 285.
[55] R.C. Newman, M.A.A. Ajjawi, Corrosion Science 26 (12) (1986) 1057–1063.
[56] Y.C. Lu, R. Bandy, C.R. Clayton, R.C. Newman, J. Electrochemical Society 130 (8) (1983) 1774–1776.
[57] C.R. Clayton, G.P. Halada, J.R. Kearns, Materials Science and Engineering A198 (1995) 135–144.
[58] G.P. Halada, D. Kim, C.R. Clayton, Paper No. 536. in: NACE/Corrosion 1995.
[59] I. Olefjord, B. Brox, U. Jevelstam, J. Electrochemical Society 132 (1985) 2854.
[60] W. Diekmann, G. Pazner, H.J. Grabke, Surface Sci. 218 (1988) 507.
[61] Y.C. Lu, J.L. Luo, M.B. Ives, Corrosion 47 (11) (1991) 835–839.
[62] M.B. Ives, Y.C. Lu, J.L. Luo, Corrosion Science 32 (1) (1991) 91–102.
[63] C.R. Clayton, Y.C. Lu, J. Electrochemical Society 133 (1986) 2465.
[64] R.F.A. Jargelius-Pettersson, SIMR Report IM-2179. 1987.
[65] R.F.A. Jargelius-Pettersson, SIMR report IM-2897. 1992.
[66] G. Bianchi, A. Cerquetti, F. Mazza, S. Torchio, Corrosion Science 10 (1970) 19–27.
[67] T. Hakkarainen, in: Proc. Electrochemical Methods in Corrosion Research, Toulouse, 1985.
[68] N. Cabrera, N.F. Mott, Rep. Progress Physics 12 (1949) 163–184.
[69] A. Charlesby, Proc. Phys. Soc. London B66 (1953) 317.
[70] M. Stern, J. Electrochemical Society 106 (5) (1959) 376–381.
[71] R. Kirchheim, B. Heine, H. Fischmeister, S. Hofmann, H. Knote, U. Stolz, Corrosion Science 29 (7) (1989) 899–917.
[72] G.T. Burstein, P.I. Marshall, Corrosion Science 23 (4) (1983) 125–137.
[73] R.F.A. Jargelius-Pettersson, B. Pound, J. Electrochemical Society 145 (5) (1998) 1462–1469.
[74] M. Pourbaix, Atlas of Electrochemical Equilibria in Aqueous Solution. Pergamon, 1966.
[75] D. Kim, C.R. Clayton, M. Oversluizen, Materials Science and Engineering A186 (1994) 163–169.
[76] R. Kirchheim, Electrochimica Acta 32 (11) (1987) 1619–1629.
[77] P.I. Marshall, G.T. Burstein, Corrosion Science 24 (5) (1984) 463–478.
[78] R.F.A. Jargelius-Pettersson, Scripta Metall. 28 (1993) 1399–1403.